

Research paper

A pan-cancer analysis of HER2 index revealed transcriptional pattern for precise selection of HER2-targeted therapy

Ziteng Li^{a,b,#}, Siyuan Chen^{a,b,#}, Wanjing Feng^{a,b}, Yixiao Luo^{a,b}, Hongyan Lai^a, Qin Li^a, Bingqiu Xiu^b, Yuchen Li^a, Yan Li^{a,b}, Shenglin Huang^{a,b,*}, Xiaodong Zhu^{a,b,*}

^a Department of Medical Oncology, Fudan University Shanghai Cancer Center, and the Shanghai Key Laboratory of Medical Epigenetics, the International Co-laboratory of Medical Epigenetics and Metabolism, Ministry of Science and Technology, Institutes of Biomedical Sciences, Fudan University, Shanghai, 200032, China

^b Department of Oncology, Shanghai Medical College, Fudan University, Shanghai, China



ARTICLE INFO

Article History:

Received 13 July 2020

Revised 29 September 2020

Accepted 30 September 2020

Available online xxx

Keywords:

HER2-amplification
HER2-enriched subtype
Pan-cancer
Biomarker
Multi-omics analysis
Machine learning

ABSTRACT

Background: The prevalence of HER2 alterations in pan-cancer indicates a broader range of application of HER2-targeted therapies; however, biomarkers for such therapies are still insufficient and limited to breast cancer and gastric cancer.

Methods: Using multi-omics data from The Cancer Genome Atlas (TCGA), the landscape of HER2 alterations was exhibited across 33 tumor types. A HER2 index was constructed using one-class logistic regression (OCLR). With the predictive value validated in GEO cohorts and pan-cancer cell lines, the index was then applied to evaluate the HER2-enriched expression pattern across TCGA pan-cancer types.

Findings: Increased HER2 somatic copy number alterations (SCNAs) could be divided into two patterns, focal- or arm-level. The expression-based HER2 index successfully distinguished the HER2-enriched subtype from the others and provided a stable and superior performance in predicting the response to HER2-targeted therapies both in breast tumor tissue and pan-cancer cell lines. With frequencies varying from 12.0% to 0.9%, tumors including head and neck squamous tumors, gastrointestinal tumors, bladder cancer, lung cancer and uterine tumors exhibited high HER2 indices together with HER2 amplification or overexpression, which may be more suitable for HER2-targeted therapies. The BLCA.3 and HNSC.Basal were the most distinguishable subtypes within bladder cancer and head and neck cancer respectively by HER2 index, implying their potential benefits from HER2-targeted therapies.

Interpretation: As a pan-cancer predictive biomarker of HER2-targeted therapies, the HER2 index could help identify potential candidates for such treatment in multiple tumor types by combining with HER2 multi-omics features. The discoveries of our study highlight the importance of incorporating transcriptional pattern into the assessment of HER2 status for better patient selection.

Funding: The National Key Research and Development Program of China; Clinical Research and Cultivation Project of Shanghai ShenKang Hospital Development Center.

© 2020 The Authors. Published by Elsevier B.V. This is an open access article under the CC BY-NC-ND license (<http://creativecommons.org/licenses/by-nc-nd/4.0/>)

1. Introduction

HER2-amplification and overexpression are important in precision medicine, as it presents an identifiable target of anti-HER2

therapies in patients of breast cancer or gastric cancer [1,2]. Since aberrant HER2 status of multiple levels have been identified in a wide range of other tumors, including uterine cancer, gastroesophageal junction cancer, biliary tract cancer, colorectal cancer, non-

Abbreviations: ACC, adrenocortical carcinoma; BLCA, bladder urothelial carcinoma; BRCA, breast invasive carcinoma; CESC, cervical squamous cell carcinoma and endocervical adenocarcinoma; CHOL, cholangiocarcinoma; COAD, colon adenocarcinoma; DLBC, lymphoid neoplasm diffuse large b-cell lymphoma; ESCA, esophageal carcinoma; GBM, glioblastoma multiforme; HNSC, head and neck squamous cell carcinoma; KICH, kidney chromophobe; KIRC, kidney renal clear cell carcinoma; KIRP, kidney renal papillary cell carcinoma; LAML, acute myeloid leukemia; LGG, brain lower grade glioma; LIHC, liver hepatocellular carcinoma; LUAD, lung adenocarcinoma; LUSC, lung squamous cell carcinoma; MESO, mesothelioma; OV, ovarian serous cystadenocarcinoma; PAA, pancreatic adenocarcinoma; PCPG, pheochromocytoma and

paraganglioma; PRAD, prostate adenocarcinoma; READ, rectum adenocarcinoma; SARC, sarcoma; SKCM, skin cutaneous melanoma; STAD, stomach adenocarcinoma; TGCT, testicular germ cell tumors; THYM, thymoma; THCA, thyroid carcinoma; UCS, uterine carcinosarcoma; UCEC, uterine corpus endometrial carcinoma; UVM, uveal melanoma; RFS, recurrence-free survival; pCR, pathological complete response

* Corresponding author.

E-mail addresses: slhuang@fudan.edu.cn (S. Huang), xddr001@163.com (X. Zhu).

These authors contributed equally to the study.

Research in Context

Evidence before this study

Therapies targeting human epidermal growth factor receptor 2 (HER2) have been routinely applied to patients of breast cancer and gastric cancer harboring HER2 alterations; such applications could be broader given the prevalence of aberrant HER2 status in multi-omics level in pan-cancer. However, the heterogeneous responses were observed in clinically HER2-positive tumors identified via IHC and/or ISH. Patient segmentation based on transcriptional profile in breast cancer identified that HER2-enriched subtype generally presented better outcome, which suggested the significance of evaluating HER2 status upon the transcriptional level as a supplement to current biomarkers.

Added value of this study

This study is novel in elucidating multi-omics features of HER2 in pan-cancer and constructing an expression-based HER2 index to evaluate the HER2-enriched transcriptional pattern across multiple tumors types harboring HER2 aberrations. With stable and superior performance in both breast tumor tissue and pan-cancer cell lines, the HER2 index could potentially act as a predictive biomarker of HER2-targeted therapies applicable to a broader range of tumor types.

Implications of all the available evidence

The trials exploring the potential value of therapeutics for HER2 have achieved some positive results in pan-cancer; however, the sample sizes of these studies are small and the criteria for HER2-positive status are various. This study demonstrated the heterogeneity of clinically HER2 positive tumors and for the first time came up with a method to refine the assessment of HER2 status via incorporating the evaluation of HER2-enriched expression pattern. The results encouraged the implementation of HER2-targeted therapies in a wider range of tumors and the consideration of transcriptional pattern for precise patient selection of future clinical trials.

biomarkers are insufficient to fully guide anti-HER2 therapies, and taking transcriptional subtypes into consideration for further stratification may be more meaningful. Furthermore, since whether transcriptional subtypes of other HER2-amplified tumors share common expression pattern with the HER2-enriched subtype hasn't been elucidated yet, the exploration of pan-cancer subtypes may gain valuable insights in extending the application of anti-HER2 therapies to a wider range of cancers.

In this study, we harnessed TCGA database to elucidate the landscape of multi-omics HER2 status in pan-cancer, and we exploited a machine learning method to evaluate the HER2-enriched expression pattern across different cancer subtypes, in order to give clues to the application of anti-HER2 therapies in a wider range of cancers.

2. Methods

2.1. Datasets

2.1.1. TCGA dataset

All TCGA datasets were downloaded from the TCGA Data Portal using "TCGAbiolinks" R package [15]. *Copy number variation data* (data.type="Gene Level Copy Number Scores"). Numeric focal-level CNV values were generated with "Masked Copy Number Segment" files from tumor aliquots using GISTIC2 on a project level [16,17]. Only protein-coding genes were kept, and their numeric CNV values were further thresholded by a noise cutoff of 0.3. for detailed HER2 SCNAs analysis, we used a binary call for CNV resulted from the level 3 segmented copy number profiles from TCGA, in which "1" represents for low-level amplification and "2" for high-level amplification. *SNV data* (pipelines="mutect2") is a modified version which removed low quality and potential germline variants. Samples harbored mutations in ERBB2 were labeled as "mutation", while the rest were labeled as "wild". *Gene expression data* (data.type="Gene Expression Quantification", workflow.type="HTSeq-FPKM"). RNA-Seq expression level read counts produced by HT-Seq are normalized using FPKM (Fragments per Kilobase of transcript per Million mapped reads). *Clinical data and clinical HER2 positivity*. Clinical HER2 positivity was assessed by TCGA following the American Society of Clinical Oncology (ASCO)/College of American Pathologists (CAP) guidelines for IHC, supplemented with fluorescent in-situ hybridization (FISH) results and/or copy number calls for tumors with equivocal or missing HER2 IHC. *RPPA data*. Level-3 RPPA data were downloaded using "RTCGAToolbox" R package [18].

2.1.2. GEO Datasets

All the GEO datasets were downloaded using "GEOquery" R package [19]. Five cohorts "GSE81002", "GSE22358", "GSE20194", "GSE50948", and "GSE55348" were utilized to validate the performance of HER2 index in separating HER2-enriched subtype from other samples of BRCA. "GSE50948" and "GSE55348" were further used for the evaluation of HER2 index in predicting the response of BRCA to trastuzumab-contained regimens under the neoadjuvant and adjuvant setting. The detailed information of these datasets could be accessed in the Supplementary Table 5.2. BRCA "GSE86166", "GSE3494", "GSE2034", STAD "GSE62254", "GSE84426", "GSE26899", "GSE26901", colorectal cancer "GSE39582", "GSE14333", "GSE37892", BLCA "GSE32894", "GSE13507" and lung cancer "GSE41271", "GSE68465", "GSE37745", "GSE31210", "GSE30219", "GSE50081" dataset were exploited to explore the prognostic performance of our index across pan-cancer tumor types (Figure S11).

2.1.3. Cell line drug sensitivity data

The log-transformed IC50 data of pan-HER inhibitors of 922 pan-cancer cell lines was acquired from Genomics of Drug Sensitivity in Cancer (GDSC) database [20]. The corresponding cell line genomic data was downloaded from GDSC1000 resource (<https://www.gdsc.org/>).

small-cell lung cancer and bladder cancer [3], its application may be far beyond than the current. Incidences of HER2 aberration differed from study to study, and since HER2-overexpression is not restrictedly due to HER2-amplification [4], its status varies among different omics levels [3]. In breast cancer, anti-HER2 therapies currently is only applied to clinical HER2-positive patients that are assessed via in situ hybridization (ISH) and immunohistochemistry (IHC) assays [5]. However, these targeted therapies only eradicated approximately 50% of HER2-positive tumors of early status and failed to cure those have metastasized [6].

Transcriptional profiling has enabled many cancers to be classified into distinct transcriptional subtypes, such as the PAM50 subtypes of breast cancer, including luminal A and B, basal and HER2-enriched subtypes [7]. These four intrinsic subtypes have showed different clinical outcomes and responses to anti-HER2 therapies [8–10], in which the HER2-enriched subtype benefited most from trastuzumab, followed which were luminal A and B subtypes, and the basal-like subtype benefited least in all HER2-amplified tumors [11–14]. Besides, the HER2-enriched subtype also showed capacity in identifying responders to dual HER2 blockade therapies in HER2-positive patients of breast cancer, of which 41% achieved pathological complete response (pCR) at the time of surgery, compared to 10% in other subtypes [12]. These results strongly indicate that the current

cancerrxgene.org/gdsc1000/GDSC1000_WebResources/Home.html). The pan-HER inhibitors include Lapatinib, Afatinib and Sapitinib. Lapatinib and Afatinib target both ERBB2 and EGFR whereas Sapitinib inhibits EGFR, ERBB2 and ERBB3.

2.1.4. Genetic dependency data

We downloaded genetic dependency dataset that contains genome-scale CRISPR knockout results of 17,634 genes of primary pan-cancer cell lines [21,22]. The median dependency score of genes essential for cell survival is -1, while the median score for genes non-essential for cell survival is 0.

2.1.5. Cell line genomics data and annotations

Cancer cell line genomic data used for genetic dependency analysis were downloaded from depmap (<https://depmap.org/portal/download/>) [23,24]. Annotations of primary disease site and disease subtype for each cell line were downloaded from the Cancer Cell Line Encyclopedia (CCLE) database (<https://portals.broadinstitute.org/ccle/data>). Gene level copy number data is generated by mapping genes onto the segment level calls, followed by log₂-transformed with a pseudo count of 1.

2.2. Thresholds for HER2-overexpression

HER2 positivity as a standard to calculate thresholds of HER2-overexpression upon different levels (mRNA, protein and phosphoprotein). The thresholds were defined as the cutoff values maximized the concordance with clinical HER2 status. Sensitivities and specificities were calculated using “pROC” R package. Area under the curve (AUC) and confidence intervals (CI) were calculated for each ROC curve. The final cutoff values were determined as the thresholds reaching the max sum of sensitivity and specificity to distinguish clinical HER2 positive cases from the negative cases. Final results of thresholds are available in Supplementary Table 2.

2.3. Gene set variation analysis (GSVA)

GSVA was implemented using the “GSVA” R package (3.8), using hallmark and C5 gene sets (KEGG, BIOCARTA and REACTOME gene sets) from MSigDB [25,26]. GSVA results were available in Supplementary table 3. Detailed information about GSVA is available in a previous study [27].

2.4. OCLR and HER2 index construction

We first compared the HER2-enriched subtype with other three subtypes (Basal-like/Luminal A/ Luminal B), the normal-like subtype was excluded for it is considered as an artifact of having few tumor cells and abundant normal breast and/or stromal cells [12,28]. 1818 significantly DEGs (adjust. $p < 0.05$ and $|\log_2(\text{FC})| \geq 2$) were obtained, in which 857 were up-regulated and 961 were down-regulated (Supplementary table 4.1). The 857 up-regulated genes were significantly enriched in “SMID BREAST CANCER ERBB2 UP” and “NIKOLSKY BREAST CANCER 17Q11 Q21 AMPLICON” gene sets (Supplementary table 4.2). These DEGs were then used as features for model training. After scaling the corresponding expression values of HER2-signature genes via the Z-score normalization, we applied the one-class logistic regression (OCLR) machine-learning algorithm [29] to extract transcriptional features of the HER2-enriched subtype. The OCLR algorithm was performed using “gelnet” R package and yielded a weighted HER2 signature (Supplementary table 4.3). The HER2 index was defined as the Spearman correlation between Z-score transformed mRNA expression matrix and the weighted HER2 signature according to a previous study [30]. The performance was evaluated via the leave-one-out cross-validation, and the AUC score was calculated to capture the probability that a sample withheld from the

HER2+ class was scored higher than a sample from the rest classes. The average AUC was 0.979 in the training cohort (Supplementary Table 4.7).

2.5. Fast Gene Set Enrichment Analysis (FGSEA)

fgsea was performed using “fgsea” R package (Version 1.10.0). The package implements an algorithm for fast gene set enrichment analysis which allows to make more permutations and get more fine grained p-values, enabling to use accurate standard approaches to multiple hypothesis correction [31].

2.6. Signatures selected for comparison

Several expression-based biomarkers reported as the predictor of response to HER2-targeted therapies were selected for the comparison with our index [32–38] (Supplementary Table 5.3). The signatures comprise of the traditional PAM50 subtype (dichotomized as HER2-enriched and non-HER2-enriched), individual genes including ERBB2, ESR1 and PTEN as well as 8 other signatures involved in E2F1/E2F2-associated pathway (Rb.sig), AP-2 γ -regulated pathway (TFAP2C), stroma reactivation (Stroma), tumor-initiating potential (HTICs), STAT3 pathway (STAT3) and the immune response (Immune2, Immune3, T cell). Each signature was calculated as described in the original literature.

2.7. TumorMap

The UCSC TumorMap is a novel interactive visualization and analysis portal to explore patterns among tumor samples, in which the position of each sample is arranged on a hexagonal grid based on their molecular profile similarity to one another in the original genomic space. We used HER2 signature profile (1818 genes) of 6830 tumor samples of 24 cancer types comprising 96 subtypes as the layout input, and the cancer type, subtype and HER2 index of each sample as color attributes. Detailed information about TumorMap is available at <https://tumormap.ucsc.edu>.

2.8. Statistical analyses

Continuous variables were compared using the Student's t-test. Variables with an abnormal distribution were compared using Mann-Whitney U test. The efficiency of the classifier was evaluated by the receiver operating characteristic (ROC) analysis using “pROC” R package. Survival analysis was performed using the Kaplan-Meier method and the log-rank test. Univariate and multivariate Cox proportional hazards regression analysis were used to study the predictive utility of signatures on RFS. Univariate and multivariate logistic regression analysis were applied to evaluating the capabilities of multiple models in predicting pCR rate of HER2 inhibitor-containing regimens and the area under the curve (AUC) of was then used to compare the predictive performance among signatures. The statistical significance threshold was set at 0.05, if not specifically mentioned. False discovery rate (FDR) calculated via Benjamin-Hochberg procedure was provided along with the raw p-value for multiple testing correction while assessing the prognostic value of the HER2 index across pan-cancer types. All statistical analyses were implemented using the R language environment software (ver. 3.6.1). All data involved in this study is available in Supplementary table 1.

2.9. Role of funders

We claimed that the funders have no roles in study design, data collection, data analysis, interpretation or the writing of this report.

3. Results

3.1. Landscape of multi-omics HER2 status in pan-cancer

We investigated HER2 status of 11020 tumor samples from the TCGA database, encompassing 33 cancer types in aspect of copy number variation (CNV), single nucleotide variant (SNV), mRNA, reverse phase protein and phospho-protein array data (RPPA). Clinical HER2-positivity information of breast invasive carcinoma (BRCA) was utilized as standards to evaluate HER2-overexpression in pan-cancer (Fig. S1; Methods).

HER2-amplification/overexpression were prevalent across multiple cancers (Fig. 1A; Table 1). Apart from BRCA and stomach adenocarcinoma (STAD), eleven other cancers with relatively high frequencies of HER2-amplification or -overexpression were identified, including bladder urothelial carcinoma (BLCA), cervical squamous cell carcinoma and endocervical adenocarcinoma (CESC), colon adenocarcinoma (COAD), esophageal carcinoma (ESCA), lung squamous cell carcinoma (LUSC), lung adenocarcinoma (LUAD), ovarian serous cystadenocarcinoma (OV), pancreatic adenocarcinoma (PAAD), rectum adenocarcinoma (READ), uterine corpus endometrial carcinoma (UCEC), and uterine carcinosarcoma (UCS). Among these HER2-aberrant cancers, though HER2 mRNA or protein expressions reached extreme high levels in LUSC and LUAD, their fractions were merely small. While UCS had a high fraction of HER2-overexpression, their expressions were low (Fig. 1a-b).

Different levels of HER2 status significantly correlated with each other in pan-cancer, in which HER2 protein and phospho-protein exhibited the best (protein/phospho-protein: Spearman $r = 0.61$, $p < 2.2e-16$; mRNA/protein: Spearman $r = 0.475$, $p < 2.2e-16$; mRNA/phospho-protein: Spearman $r = 0.524$, $p < 2.2e-16$). Better correlations were obtained when cases without HER2-overexpression were excluded (Figure S2). Significant correlations also revealed between clinical HER2 rank tested by IHC and HER2 mRNA (Spearman $r = 0.61$, $p < 2.2e-16$), protein (Spearman $r = 0.48$, $p < 2.2e-16$) and phospho-protein (Spearman $r = 0.54$, $p < 2.2e-16$) (Figure S3). HER2-positive samples significantly enriched HER2-amplification ($p < 2.2e-16$, Chi-squared test; Figure S4). In addition, lymph node metastasis level was positively associated with HER2 mRNA (Spearman $r = 0.15$, $p = 0.0056$), protein (Spearman $r = 0.14$, $p = 0.013$) and phospho-protein (Spearman $r = 0.16$, $p = 0.0041$).

HER2-overexpression was not restrictedly limited to HER2-amplification, and discordance between genome and proteome was observed in several cancer types. A certain group of tumors with high HER2 protein and phospho-protein expressions was observed in HNSC, GBM, THCA, LGG and a part of LUSC and LUAD. Nevertheless, these cases lacked HER2-amplification or mRNA-overexpression. Moreover, several tumors of KIRP, PRAD, PAAD, SARC and partial COAD only harbored overexpressed HER2 protein (Fig. 1a and 1c). Though HER2-mutation, also prevalent in pan-cancer, was concurrent with HER2-amplification/overexpression in several cases, it was primarily independent from HER2-amplification/overexpression (Fig. 1d).

3.2. Genomic characteristics of tumors with increased HER2 SCNA in pan-cancer

HER2 is an oncogene targeted by somatic copy-number alterations (SCNAs) to drive cancer growth. For a diploid genome, SCNA occurs as long as the copy number is not equal to 2, and SCNA generally includes low-level and high-level amplification [39]. Thus we did a more detailed analysis on HER2 SCNAs (Methods).

We initially evaluated the overall intensity of SCNAs in pan-cancer, using percentage of the genome altered (PGA) for comparison. As for pan-cancer analysis, PGAs were significantly higher in HER2-amplified tumors (56.64% vs 31.03%, $p < 2.2e-16$, t-test). In individual

cancer analysis, PGAs were also consistently higher in HER2-amplified tumors in each cancer type. Notably, the thirteen HER2-aberrant cancers mentioned above gained overall higher levels of PGAs (Fig. 2a). Focusing on the chromosome 17 (Chr17) where HER2 located, PGAs of Chr17 were extremely high in tumors with increased HER2 SCNAs, with an average PGA of 90.42%. By comparison, in tumors without increased HER2 SCNAs, the average of PGAs was only 23.33% (Fig. 2a). This finding suggested the intrinsic variation of intensities of SCNA among different tumor types and a strong correlation between HER2-amplifications and genomic instability, especially upon Chr17.

While HER2 high-level amplification occurred in a low frequency, low-level amplification appeared more prevalently in pan-cancer (Fig. 2b). Apart from that, patterns of frequency of low SCNA and frequency of high SCNA of each gene on Chr17 were different. While the high SCNA pattern on Chr17 was characterized by HER2 high-level amplification with several co-amplified genes within a focal region, known as the HER2 amplicon, but with a low frequency. The low SCNA pattern was characterized by HER2 low-level amplification with a broader region of co-amplified genes (near the size of a chromosome arm), which presented with a high frequency (Fig. 2b). The HER2 amplicon was determined as a 6-gene area including *PGAP3-ERBB2(HER2)-MIR4728-MIEN1-GRB7-IKZF3*. These genes co-amplified in more than 95% HER2-amplified tumors in pan-cancer (Fig. 2c).

Since HER2 were targeted by both focal and broad SCNAs, we then explored whether high-level amplification/focal and low-level amplification/broad events had different consequences. Focal-amplification at the HER2 gene is associated with overexpressed HER2 mRNA, whereas arm-level gain had little influence on HER2 mRNA expression (Figure S5). Though we found several outliers in tumors without HER2-amplification, their SCNA patterns were the same as the focal-amplification pattern (Figure S6). Moreover, we observed divergence that SCNAs of the Chr17q22-23 subregion of Chr17 showed a higher amplification frequency in gynecologic tumors, such as BRCA (Fig. 2d), CESC, UCEC (Figure S7), compared to those of gastrointestinal tumors, such as STAD (Fig. 2d), ESCA, COAD and READ (Figure S7), suggesting Chr17q22-23 is selectively amplified in gynecologic tumors.

3.3. Transcriptomic heterogeneity of clinical HER2-positive BRCA

Different therapeutic responses have been observed in HER2-positive patients, indicating the underlying molecular diversity. We next investigated 75 clinical HER2-positive BRCA samples classified by PAM50 [7]. 51.4 percent of samples was HER2-enriched subtype, and Luminal A, Luminal B and Basal-like subtypes accounted for 18.9%, 27% and 2.7%, respectively (Fig. 3a). Nearly all HER2-enriched samples harbored HER2-amplification, and frequencies of HER2-amplification were lower in LuminalA/B and Basal-like subtypes (Fig. 3a). Besides, HER2-enriched subtype also displayed highest levels of HER2 mRNA, protein and phospho-protein (Fig. 3b).

We next performed gene set variation analysis (GSVA) to identify pathway alterations associated with each subtype, using hallmark and C5 gene sets (KEGG, BIOCARTA and REACTOME gene sets) from MSigDB [25,26]. Tumors of HER2-enriched subtype were characterized by vigorous metabolic activity, for signals of glycolysis pathway, HIF pathway etc. were significantly enhanced. Luminal A subtype was strongly related to enhanced ER response, PI3K cascade, GATA3 pathway, downstream signaling of activated FGFR etc. Luminal B was associated with elevated cell proliferation, in which cell cycle mitotic, G2-M transition, P53 pathway etc. were up-regulated. The number of Basal-like tumors were too few (2 samples) to enrich any significant pathway (Fig. 3c). The varied biological features were further validated in an external cohort (GSE81002, Figure S8). We next specifically analyzed the activity of HER2 signaling pathway in each subtype. Consensus clustering of the pairwise correlation of 217

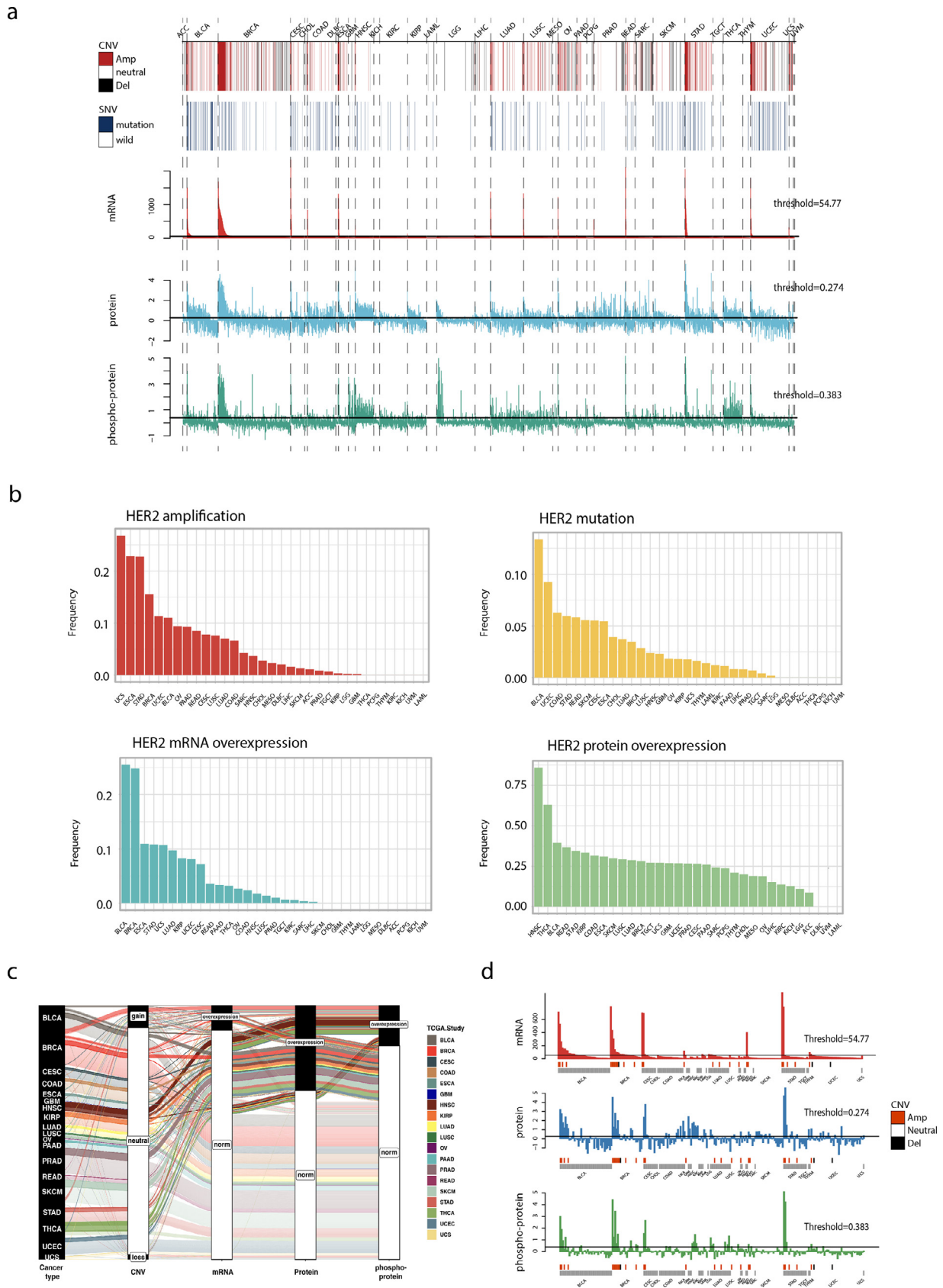


Fig. 1. Landscape of multi-omics HER2 status in pan-cancer. **a.** Multi-omics features of HER2 in 33 TCGA cancer types, including CNV, SNV, mRNA, protein and phospho-protein of HER2. Each column represents a tumor sample, for CNV and SNV, colors indicate different HER2 status; for mRNA, protein and phospho-protein, heights of the bar stands for expression levels. Thresholds are marked with black lines through bars in which bars exceeding the line are regarded as HER2-overexpression. Cancer types are separated by dash lines and labeled at the top, in which HER2- targetable cancers are in bold. **b.** Frequencies of HER2 aberrations upon CNV, SNV, mRNA, protein and phospho-protein levels in pan-cancer. **c.** Sankey plot of multi-omics HER2 status in pan-cancer. **d.** Multi-omics HER2 status of tumors with HER2 mutation in pan-cancer

Table 1
Frequencies of HER2-amplification/overexpression across 33 TCGA tumor types.

Cancer types	CNV					SNV				mRNA				RPPA				RPPA_P			
	Amp	Neutral	Del	SUM	Freq	Mut.	Wild	SUM	Freq	Over.	Norm	SUM	Freq	Over.	Norm	SUM	Freq	Over.	Norm	SUM	Freq
UCS	15	38	3	56	27%	1	56	57	2%	6	50	56	11%	13	35	48	27%	5	43	48	10%
ESCA	42	138	4	184	23%	10	174	184	5%	18	146	164	11%	39	87	126	31%	20	106	126	16%
STAD	100	337	3	440	23%	26	411	437	6%	41	339	380	11%	123	234	357	34%	58	299	357	16%
BRCA	169	876	44	1089	16%	34	952	986	3%	271	821	1092	25%	251	636	887	28%	152	735	887	17%
UCEC	61	459	19	539	11%	49	481	530	9%	45	510	555	8%	118	322	440	27%	45	395	440	10%
BLCA	45	360	5	410	11%	55	357	412	13%	104	304	408	25%	136	208	344	40%	53	291	344	15%
OV	55	493	37	585	9%	8	428	436	2%	10	366	376	3%	80	346	426	19%	33	393	426	8%
PAAD	17	167	0	184	9%	2	176	178	1%	6	171	178	3%	32	91	123	26%	10	113	123	8%
READ	14	151	0	165	8%	8	129	137	6%	6	161	167	4%	48	83	131	37%	15	116	131	11%
CESC	23	269	3	295	8%	16	273	289	6%	22	282	304	7%	46	127	173	27%	27	146	173	16%
LUSC	38	450	15	503	8%	14	478	492	3%	7	494	501	1%	96	232	328	29%	55	273	328	17%
LUAD	36	474	7	517	7%	21	546	567	4%	50	465	515	10%	105	260	365	29%	77	288	365	21%
COAD	30	420	2	452	7%	25	374	399	6%	11	445	456	2%	114	246	360	32%	55	305	360	15%
SARC	11	220	29	260	4%	1	236	237	0%	1	258	259	0%	54	169	223	24%	27	196	223	12%
HNSC	19	497	6	522	4%	12	496	508	2%	9	492	501	2%	182	30	212	86%	140	72	212	66%
CHOL	1	34	1	36	3%	2	49	51	4%	0	36	36	0%	6	24	30	20%	2	28	30	7%
MESO	2	85	0	87	2%	0	82	82	0%	0	86	86	0%	12	51	63	19%	7	56	63	11%
DLBC	1	47	0	48	2%	0	37	37	0%	0	48	48	0%	0	33	33	0%	0	33	33	0%
LIHC	6	353	16	375	2%	3	361	364	1%	1	370	371	0%	28	156	184	15%	5	179	184	3%
SKCM	6	453	11	470	1%	26	441	467	6%	0	468	468	0%	106	247	353	30%	28	325	353	8%
ACC	1	82	7	90	1%	0	92	92	0%	0	79	0	0%	4	42	46	9%	6	40	46	13%
PRAD	4	478	15	497	1%	4	491	495	1%	5	490	495	1%	94	258	352	27%	12	340	352	3%
TGCT	1	147	2	150	1%	1	143	144	1%	1	149	150	1%	32	86	118	27%	4	114	118	3%
KIRP	1	288	0	289	0%	5	276	281	2%	24	265	289	8%	72	143	215	33%	25	190	215	12%
LGG	1	509	5	515	0%	1	507	508	0%	0	511	511	0%	47	383	430	11%	40	390	430	9%
GBM	1	576	19	596	0%	9	384	393	2%	0	166	166	0%	64	174	238	27%	71	167	238	30%
KICH	0	66	0	66	0%	0	66	0	0%	0	66	66	0%	8	55	63	13%	1	62	63	2%
KIRC	0	532	0	532	0%	4	332	336	1%	3	527	530	1%	66	412	478	14%	65	413	478	14%
LAML	0	192	2	194	0%	2	141	143	1%	0	151	0	0%	NA	NA	NA	NA	NA	NA	NA	NA
PCPG	0	154	11	165	0%	0	179	179	0%	0	179	179	0%	19	61	80	24%	5	75	80	6%
THCA	0	505	0	505	0%	0	492	492	0%	16	486	502	3%	140	82	222	63%	98	124	222	44%
THYM	0	123	1	124	0%	2	121	123	2%	0	119	119	0%	19	71	90	21%	1	89	90	1%
UVM	0	78	2	80	0%	0	80	80	0%	0	80	80	0%	0	12	12	0%	0	12	12	0%

LAML: Acute Myeloid Leukemia; ACC: Adrenocortical carcinoma; BLCA: Bladder Urothelial Carcinoma; LGG: Brain Lower Grade Glioma; BRCA: Breast invasive carcinoma; CESC: Cervical squamous cell carcinoma and endocervical adenocarcinoma; CHOL: Cholangiocarcinoma; COAD: Colon adenocarcinoma; ESCA: Esophageal carcinoma; GBM: Glioblastoma multiforme; HNSC: Head and Neck squamous cell carcinoma; KICH: Kidney Chromophobe; KIRC: Kidney renal clear cell carcinoma; KIRP: Kidney renal papillary cell carcinoma; LIHC: Liver hepatocellular carcinoma; LUAD: Lung adenocarcinoma; LUSC: Lung squamous cell carcinoma; DLBC: Lymphoid Neoplasm Diffuse Large B-cell Lymphoma; MESO: Mesothelioma; OV: Ovarian serous cystadenocarcinoma; PAAD: Pancreatic adenocarcinoma; PCPG: Pheochromocytoma and Paraganglioma; PRAD: Prostate adenocarcinoma; READ: Rectum adenocarcinoma; SARC: Sarcoma; SKCM: Skin Cutaneous Melanoma; STAD: Stomach adenocarcinoma; TGCT: Testicular Germ Cell Tumors; THYM: Thymoma; THCA: Thyroid carcinoma; UCS: Uterine Carcinosarcoma; UCEC: Uterine Corpus Endometrial Carcinoma; UVM: Uveal Melanoma; Amp: amplification; Del: deletion; Mut.: mutation; Over.: overexpression

BIOCARTA pathways was performed separately for each subtype (Basal-like subtype was excluded due to lack of samples). While “Biocarta_her2_pathway” associated with a large number of other pathways in HER2-enriched subtype, less associations were observed in the other two subtypes (Fig. 3d). These results support that the activity of HER2 signaling and therapeutic responses are associated with transcriptional status, and HER2-enriched subtype exhibits the optimal subtype for anti-HER2 therapies.

3.4. Construction of HER2 index

Currently, HER2-amplification or overexpression tested by ISH or/and IHC assays is considered as the main biomarker for anti-HER2 therapies. However, research has been reported that PAM50 molecular subtype may be a better predictor [12]. Tumors of HER2-enriched subtype exhibit similar profile as that of HER2-amplified tumors, even though they lack amplification in HER2 gene [7]. Compared to the upstream genomic events, evaluation of transcriptional profile reflects the phenotype and biological behavior of different tumors. Therefore, we harnessed one-class logistic regression (OCLR) algorithm to extract transcriptomic features of the HER2-enriched subtype [29]. The model was trained on HER2-enriched BRCA from TCGA (58 samples), and produced a weighted 1818-gene signature. To explain the 1818-gene signature, we further applied fast gene set

enrichment analysis (fgsea). As expected, HER2-related pathways (PI3K, ERBB2 signaling, EGFR signaling pathways) and pathways representing for cell proliferation were significantly positive-enriched (Fig. 4c). In addition, immune-related IFN-gamma response and adaptive immune system pathways were also positively enriched, representing for an enhanced immune response. In contrast, estrogen response was negative-enriched, since ER was the driver of luminal subtypes. Moreover, TNF- α signaling via NF- κ B and Wnt pathway were also negative-enriched (Fig. 4c).

This 1818-gene signature was then harnessed to build a HER2 index (Methods). Basically, a higher HER2 index indicates a closer connection with the HER2-enriched expression pattern (Fig. 4a). The performance of the HER2 index was evaluated using leave-one-out cross-validation (Methods). The average AUC in TCGA training cohort was 0.979 with a cutoff of 0.6870 to get the highest youden index. Several external cohorts were used for validation, with all exhibiting AUCs nearly or more than 0.9, confirming the remarkable value of HER2 index separating HER2-enriched subtype from other subtypes of BRCA (Methods, Figure S9, Supplementary Table5.2). HER2 index was positively associated with expressions of HER2 mRNA, protein, and phosphorylated protein (Fig. 4b). Besides, HER2 index was significantly higher in HER2-amplified tumors (the average is 0.712 for of Amp, and 0.41 for Neutral) and clinical HER2-positive cases (the average is 0.752 for HER2+, and 0.409 for HER2-). As for clinical features,

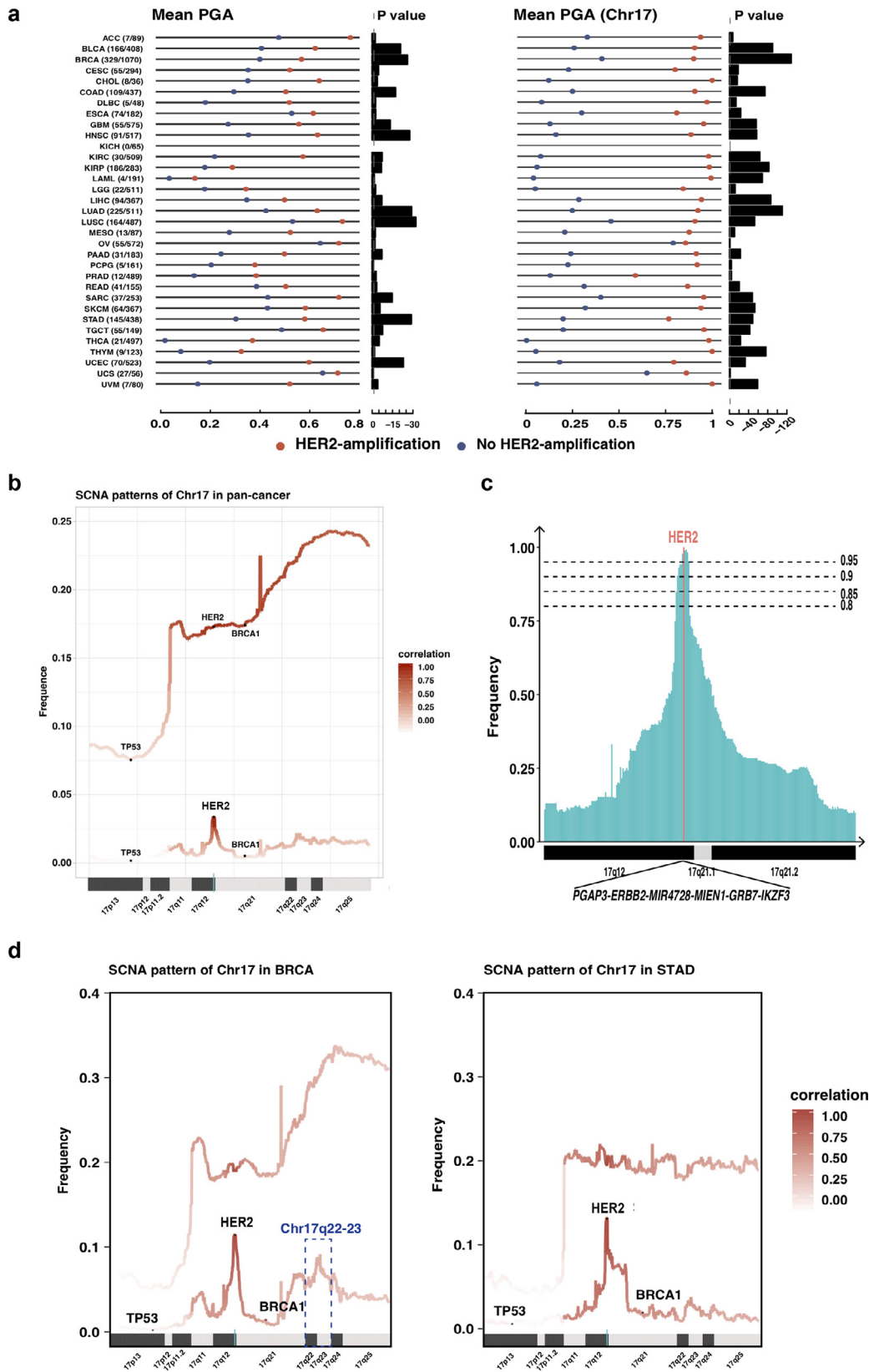


Fig. 2. Genomic characteristics of tumors with increased HER2 SCNA in pan-cancer. **a.** Comparisons between PGAs of tumors with and without HER2-amplification in pan-cancer (left: PGAs of the whole genome; right: PGAs of Chr17). **b.** SCNA patterns of Chr17 in pan-cancer. X axis and y axis represent for gene location on the Chr17 and its amplification frequency, respectively. The upper line indicates for tumors with low-level HER2 amplification, and the bottom line indicates for tumors with high-level HER2 amplification. The color intensity of each dot on the upper line suggests for the association between low-level SCNA status of this specific gene with low-level HER2 SCNA status. While the color intensity of each dot on the bottom line suggests for the association between high-level SCNA status of this specific gene with high-level HER2 SCNA status. **c.** HER2 amplicon. X axis and y axis represent for gene location on the Chr17q and its amplification frequency in HER2-amplified tumors, respectively. Six genes including PGAP3, ERBB2(HER2), MIR4728, MIEN1, GRB7 and IKZF3 co-amplified in over 95% HER2-amplified tumors. **d.** Comparisons of 12 SCNA patterns of Chr17q22-23 in BRCA and STAD, indicating Chr17q22-23 is selectively amplified in gynecologic tumors.

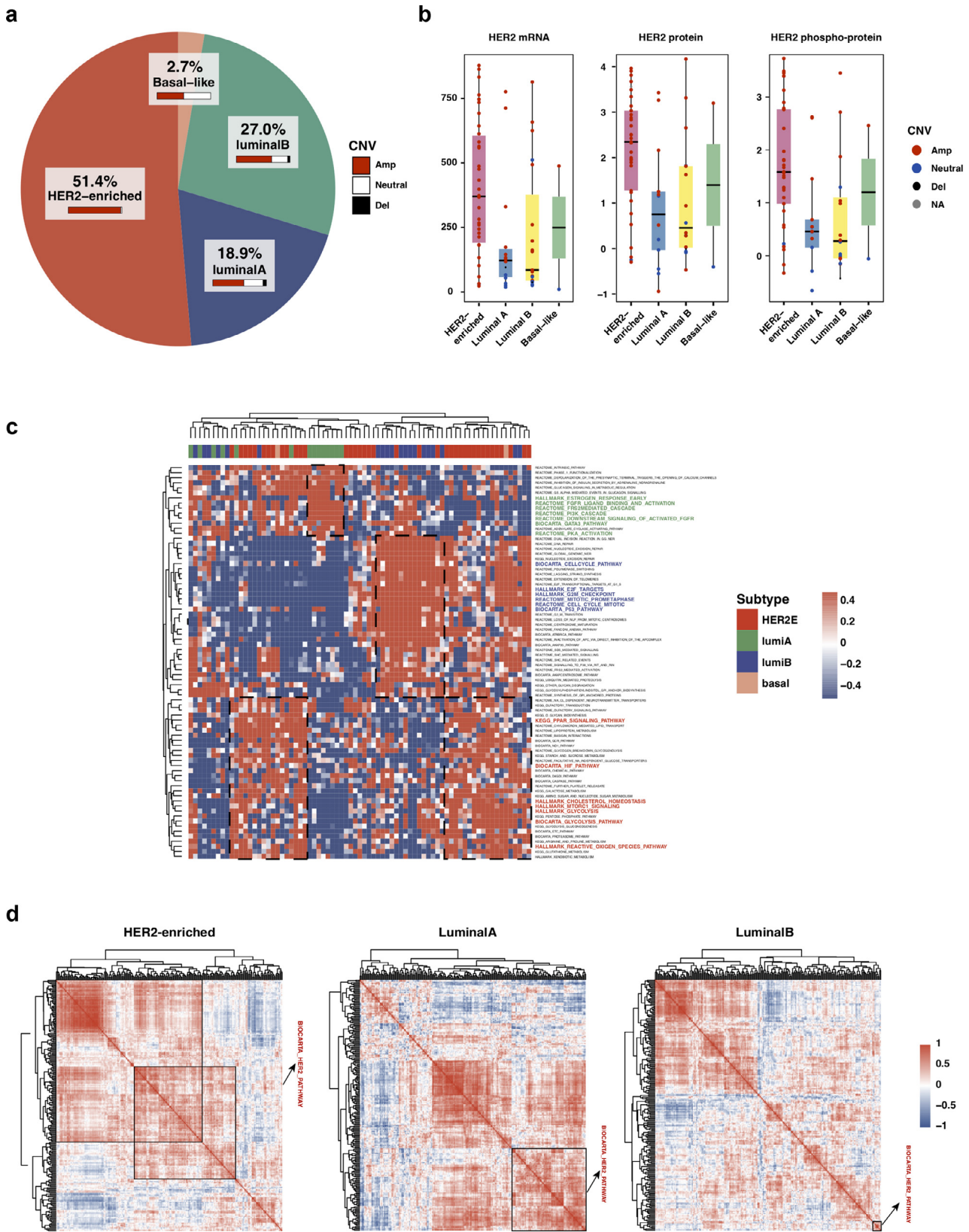
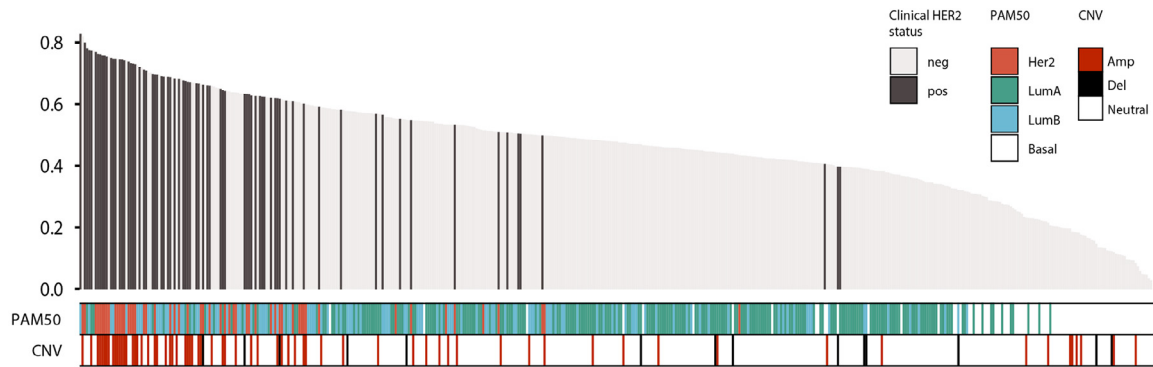


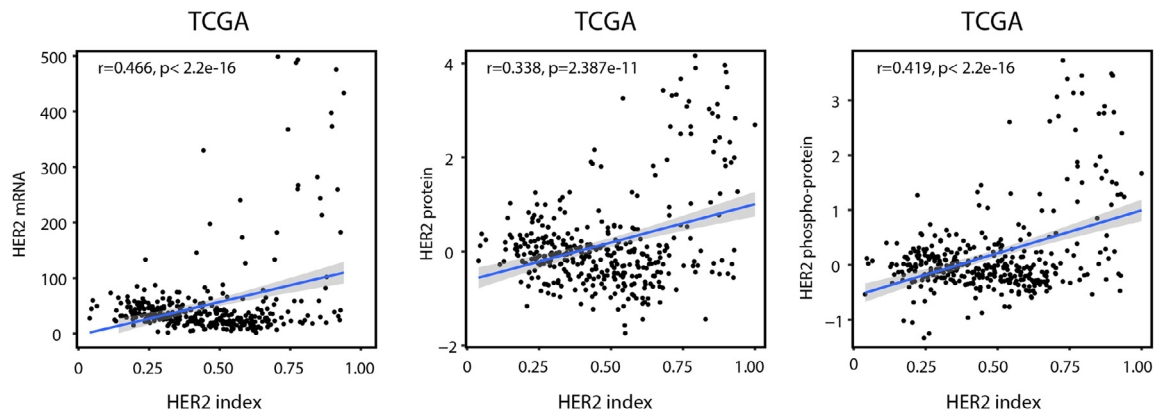
Fig. 3. Transcriptomic heterogeneity of clinical HER2-positive BRCA. a. Fractions of four intrinsic subtypes of 75 clinical HER2-positive BRCA samples. Fraction of different HER2-CNV status in each subtype are displayed using horizontal bars. b. Comparisons of HER2 mRNA, protein and phosphor-protein among four intrinsic subtypes. c. Clustering heatmap using differential expressed pathways identified by GSVA. Subtype of each sample is annotated at the top. d. Consensus clustering of the pairwise correlation of HER2 pathway and 216 BIOCARTA pathways in HER2-enriched, Luminal A and Luminal B subtypes.

a

HER2 index in TCGA training cohort



b



c

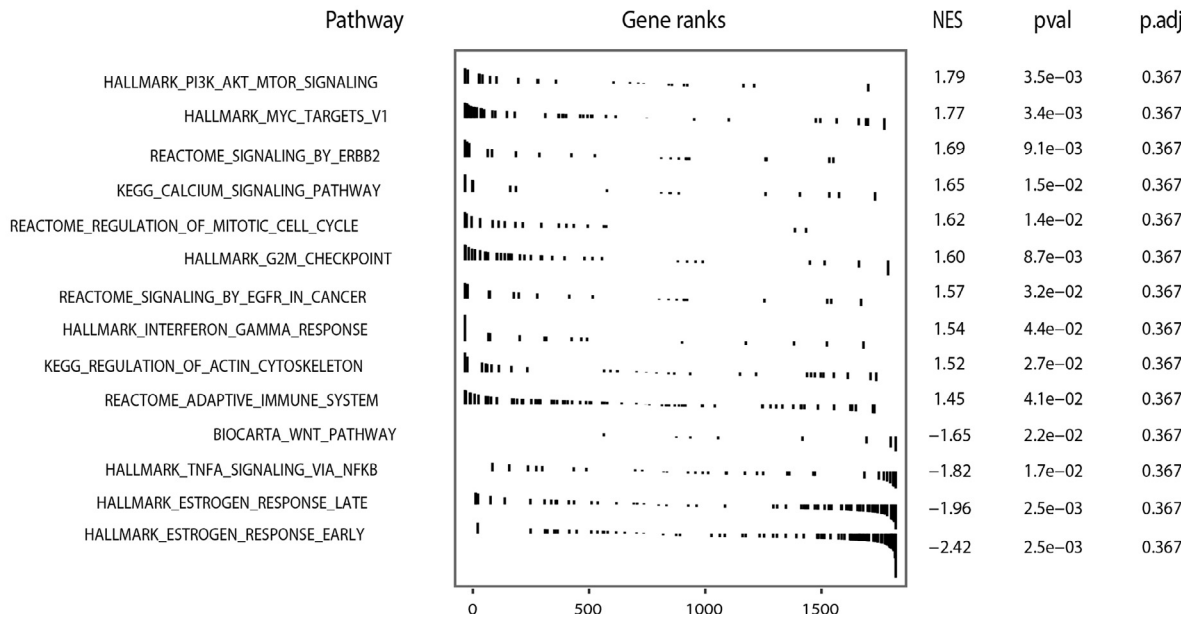


Fig. 4. Construction of HER2 index using machine learning. a. HER2 index of TCGA training cohort derived using HER2 signature. Each bar represents a single tumor sample in BRCA, with height standing for HER2 index and color indicating the corresponding subtype. The HER2 index was defined as Spearman correlation between mRNA expression matrix and weighted HER2 signature. The performance was evaluated via leave-one-out cross-validation, and the average AUC of TCGA training cohort was 0.979. b. Correlations between HER2 index and expressions of HER2 mRNA, protein and phospho-protein (Spearman). c. fgsea. HER2 signature was compared with hallmark gene sets, C2 gene sets (KEGG, BIO-CARTA and REACTOME pathways) and C5 gene sets (GO-BP level) from MSigDB.

HER2 index was related to larger tumor size (Spearman $r = 0.19$, $p = 0.0002$), more lymph nodes metastasis (Spearman $r = 0.113$, $p = 0.03$) and higher tumor stage (Spearman $r = 0.164$, $p = 0.0016$, Supplementary Table 4.4).

3.5. The predictive value of HER2 index over the response to HER2-targeted therapy

To further validated that our HER2 index was able to predict the response to HER2-targeted therapies, we initially evaluated its predictive performance in two independent GEO cohorts (GSE55348, GSE50948, Methods). Both cohorts contained patients with HER2-positive breast tumor and receiving trastuzumab-based treatment, of which the recurrence-free survival (RFS) and pCR rate could be used for the measurement of response, respectively. We have also selected several signatures reported to be predictive in the existing works, including traditional PAM50 subtype, three individual genes and eight other metagenes for the comparison with our index (Methods). Assessed in the adjuvant setting, multiple signatures exhibited significant capacities of identifying responders with better RFS including HER2 index, the mRNA expression of ERBB2 and ESR1, Rb-related signature, immune 2 as well as the T cell metagene (Fig. 5b). However, it is suggested that our index was the only significant predictor of pCR rate with a higher AUC against other signatures tested in both univariate and multivariate logistic regression analysis (OR = 97.862, 95%CI = 2.866–5944.302, $p = 0.017$, AUC = 0.665 in univariate; OR = 92.768, 95%CI = 1.739–8514.602, $p = 0.035$, AUC = 0.732 in multivariate with ER status, age and tumor size incorporated, Fig. 5a). The model combining our index with clinicopathological factors exhibited an AUC of 0.732 for pCR prediction. These results supported that our HER2 index could provide a more stable and superior performance as a predictive biomarker of HER2-targeted therapies in BRCA.

As anti-HER2 treatment has not been approved for use in most of solid tumors, the combined analysis of genomic profile of bulk tissue and the corresponding HER2-blocking sensitivity was almost unapproachable. In order to further evaluate the predictive value of our HER2 index across a spectrum of human malignancies, we assessed the correlation of our index with the response to pan-HER inhibitors (including lapatinib, afatinib, and sapitinib) in BRCA cell lines and pan-cancer cell lines respectively (Methods, Fig. 5d). The HER2 index exhibited a significantly negative correlation with IC50 of HER2 inhibitors in breast cancer cell lines (Spearman $r = -0.5387$, $p = 7.81 \times 10^{-5}$ for lapatinib; Spearman $r = -0.4626$, $p = 9.827 \times 10^{-9}$ for Afatinib; Spearman $r = -0.5641$, $p = 2.974 \times 10^{-5}$ for Sapitinib). Such correlations became moderate though still significant when our index was applied to pan-cancer tumor types (Spearman $r = -0.2422$, $p = 3.551 \times 10^{-11}$ for lapatinib; Spearman $r = -0.1704$, $p = 6.683 \times 10^{-18}$ for Afatinib; Spearman $r = -0.2548$, $p = 7.601 \times 10^{-13}$ for Sapitinib) and better while only including cell lines with HER2 amplifications (Figure S12), which could to some extent support the predictive value of our index over the response to HER2-blocking therapies. Considering that ERBB3 and EGFR are also targeted by these pan-HER inhibitors, we additionally acquired the genome-scale CRISPR knockout results of HER2 gene across pan-cancer cell lines from depmap (Methods) and assessed the association between HER2 index and HER2-dependency score. The results showed that pan-cancer cell lines scored high in HER2 index were more vulnerable to the knockout of HER2 gene (Spearman $r = -0.37$, $p < 2.2 \times 10^{-16}$, Figure 5c), suggesting that the HER2 index may act as a pan-cancer predictor of and help identify patients more likely to respond to HER2 inhibitors.

The prognostic value of HER2 index was also explored across 13 tumor-aberrant tumors using TCGA data and independent GEO datasets (Methods). Measured as a continuous variable, higher HER2 index was found as a significant risk factor of OS and PFS in BRCA and LUAD in both TCGA and GEO cohorts (Supplementary Table 5.1, Fig. S11a-b). The negative correlation of our index with survival in BRCA

could be due to the relative low score of luminal subtypes reported with better prognosis. Though significance was not obtained in COAD and STAD cohort of TCGA, a tendency of association with favorable survival was shown, which was in line with the discoveries in GEO datasets of corresponding tumor types (Figure S11b).

3.6. Evaluation of HER2 expression pattern in pan-cancer

Even though the location of a primary tumor dominantly contributes to gene expression pattern, commonalities across tissues can be revealed through pan-cancer comparisons. Having validated the pan-cancer predictive value of HER2-enriched expression pattern assessed by our index, we wondered whether other pan-cancer types present such pattern at some appreciable level. Therefore, we calculated HER2 index for a total of 10,192 TCGA samples, the results of which were shown in Fig. 6a. HER2 index varied among pan-cancer tumor types, with the HER2-enriched subtype of BRCA showing the highest. Though Luminal A, Luminal B and Basal-like subtypes obtained a low median of HER2 index, HER2-amplified tumors of these subtypes gained high levels of HER2 index. In the thirteen HER2-aberrant cancers, Pan-GI (ESCA/STAD/COAD/READ) cancers, HNSC, CESC, BLCA, LUSC, LUAD and UCEC generally exhibited higher HER2 index. Demonstrating a HER2-enriched expression pattern, a certain fraction of these tumors scored over the cutoff of HER2 index acquired above (0.6870), in which the multi-omics features of HER2 were further explored (Fig. 6a–b). With frequencies varying from 0.9% of UCEC to 12.0% of HNSC, these HER2-aberrant tumors showed consistent HER2 amplification or overexpression with HER2-enriched transcriptional pattern, which were more likely to benefit from HER2-targeted therapy (Table 2). In addition, some interesting findings were also notable. From the perspective of CNV, it was noteworthy that HER2-amplifications were generally enriched in pan-cancer with higher HER2 index, which was consistent with that in HER2-enriched BRCA. However, other than STAD and ESCA, other HER2-aberrant tumors with higher index were lacking in HER2-amplifications in spite of the high similarity with HER2-enriched subtype in the transcriptional aspect, which suggested that HER2-enriched pattern may be independent of HER2 amplification status. As for transcription level, the majority of HER2-aberrant tumors with high HER2 index displayed a HER2 transcription level below the cutoff ($\log_{10}(\text{HER2 mRNA cutoff}) = 1.74$). HNSC with high HER2 index had a significantly elevated HER2 protein and phosphor-protein level despite few HER2 amplifications and mRNA overexpression, coinciding with the landscape of HER2 status displayed in the total of HNSC samples (Fig. 1c). To be mentioned, nearly or over 75% of high scored COAD, READ, LUSC, CESC and UCEC showed scarce feature of HER2 overexpression in multi-omics level, additionally suggesting that HER2-enriched pattern could also be driven by alternatively activated pathway besides HER2.

To take a deeper understanding of the molecular signatures of HER2-enriched pattern in pan-cancer, we additionally calculated HER2 index separately in molecular subtypes of pan-cancer based on TCGA Research Network tumor-specific publications (Methods) (Figure S14). We primarily focused on ten types of HER2-aberrant tumor scoring relatively higher HER2 index as analyzed above and observed variations among different molecular subtypes of these cancers. Other than BRCA.Her2 subtype (HER2-enriched), HER2 amplifications were mainly enriched in GI.CIN and UCEC.CN_HIGH subtypes. However, the HER2 amplifications in UCEC.CN_HIGH subtype were weakly associated with HER2 index and this subtype ranked far lower than GI.CIN over the similarity with HER2-enriched pattern. The GI.HM-SNV, GI.HM-Indel and GI.CIN presented comparable index despite the concentration of gain of HER2 in the latter subtype (Supplementary Table 5). Besides, among HNSC tumors, basal subtype scored the highest.

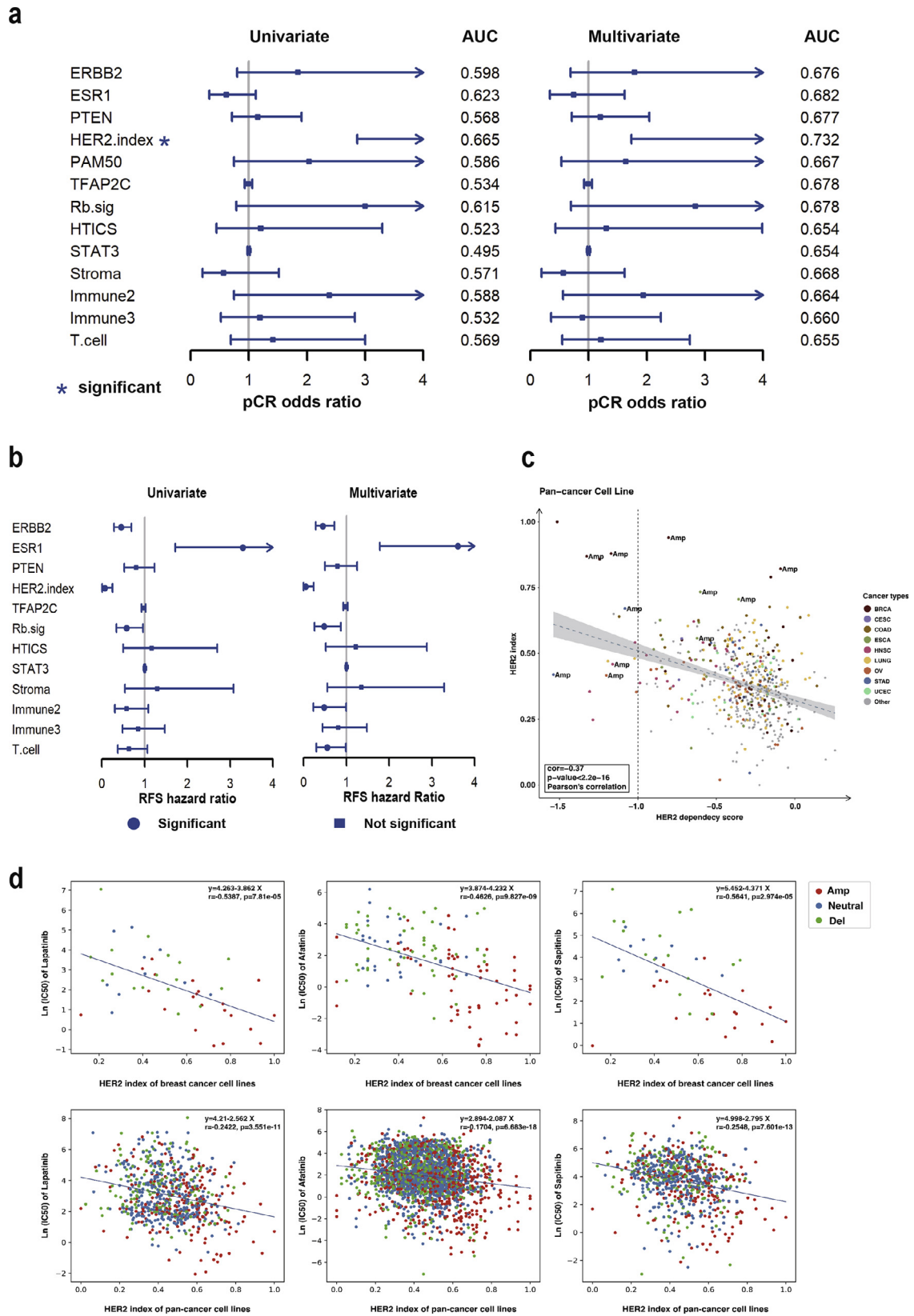


Fig. 5. The predictive value of HER2 index over the response to HER2-targeted therapy. a. The HER2 index acted as the only significant predictor of pCR rate of trastuzumab-contained neoadjuvant treatment among 13 signatures tested via both univariate (OR = 97.862, $p = 0.017$) and multivariate Cox regression analysis (OR = 92.768, $p = 0.035$) incorporated with ER status, age and tumor size (GSE50948, $n = 63$). b. Signatures including HER2 index (HR = 0.04, $p = 4.9e-4$ for univariate; HR = 0.029, $p = 0.001$ for multivariate), ERBB2 (HR = 0.44, $p = 3.5e-4$ for univariate; HR = 0.45, $p = 7.89e-4$ for multivariate) and ESR1 (HR = 3.29, $p = 3.4e-4$ for univariate; HR = 3.609, $p = 3.46e-4$ for multivariate), Rb.sig (HR = 0.57, $p = 0.034$ for univariate; HR = 0.475, $p = 0.0165$ for multivariate), Immune2 (HR = 0.475, $p = 0.0482$ for multivariate), and T.cell (HR = 0.543, $p = 0.0448$ for multivariate) exhibited significant RFS hazard ratios in patients receiving trastuzumab-contained adjuvant regimen in univariate and/or multivariate logistic analysis combined with ER status,

A further cluster analysis using TumorMap [40] based on the 1818-gene HER2 signature was performed (Methods). The TumorMap landscapes showed that HER2-targetable cancers tended to assemble together and present with high HER2 index, indicating a shared HER2-enriched expression pattern among these cancers which could be identified by our index. And we noticed that Gli.CIN, BLCA.3 and HNSC.Basal in the corresponding cancer tended to have a closer connection with the HER2-enriched subtype (Figure S15). We then explored performance of HER2 index to distinguish pan-cancer subtypes of the same tissue origin. As the HER2 index was derived from mRNA expression pattern, it should be applied within cancers of which the molecular classification was based on merely the transcriptional. We restricted cancer types to BLCA, HNSC, LUSC, OV, UCEC and UCS, and used Gli.CIN as a comparison. As a result, the HER2 index classifier could distinguish BLCA.3 (AUC: 0.71, $p = 0.0006$) and HNSC.Basal (AUC: 0.74, $p = 4.2e-10$) with satisfactory performance. By comparison, Gli.CIN failed to be distinguished by HER2 index (Fig. 6c and Figure S14b).

4. Discussion

HER2-amplification/overexpression is a successful drug-target in clinical practice, especially in breast cancer. However, it may have a more profound clinical application, due to its prevalence in pan-cancer. In this study, we elucidated the multi-omics landscape of HER2 in pan-cancer. Consistent with previous research, HER2-amplification/overexpression also occurred frequently in CESC, UCEC, OV, UCS, ESCA, COAD, READ, BLCA, LUSC, LUAD and HNSC [41]. Since some of these tumors have limited therapeutic options, in light of the successes achieved in HER2-positive breast cancer, exploring the efficacy of anti-HER2 therapies in these cancers may be prospective.

We captured several discordances between genome and proteome in that HER2-overexpression, not restrictedly derived from HER2-amplification, also occurred in absence of HER2-amplification. The downstream overexpressed HER2 protein could be interpreted by at least two mechanisms, including HER2 DNA amplification and enhanced translation [42]. HER2 mutation has been suggested as an alternative mechanism for activating HER2 signaling [43], and functional analysis have revealed several recurrent HER2 mutations that are likely to be driver alterations [44]. We found that HER2 mutations were also common in pan-cancer, but they are mainly independent from HER2-amplification. This was in line with previous researching results that somatic mutations in HER2 typically occurred in absence of amplification [45,46]. There is a small fraction of tumors having both HER2 amplification and mutation, however, whether they are same with purely HER2-amplified tumors remains uncertain. Since oncogenic potentials have been identified in HER2 mutations, amplifications and changes in HER2 protein [3] and variations in different cancers, thus identifying the significance of each alteration in the context of each cancer is needed in the future.

As HER2 is mainly targeted by SCNAs to drive tumorigenesis, we performed genomic analysis and revealed that HER2 SCNAs were strongly correlated with increased genomic instability, in which Chr17 where HER2 located obtained extremely high levels of PGA. SCNA patterns of genes on Chr17 could be divided into two distinct types. While HER2 focal amplification led to HER2 mRNA overexpression, HER2 arm gain showed little influence in HER2 mRNA expression. In a previous study, Beroukhim R, et al. has used chr7 as an example to explore the difference between broad and focal SCNA events. EGFR was overexpressed in most 7^{gain}EGFR^{amp} GBMs, but in none of the 7^{gain} GBMs in the absence of focal EGFR-amplification.

Functional analysis elucidated distinct consequences of 7^{gain}EGFR^{amp} and 7^{gain} GBMs. While 7^{gain}EGFR^{amp} GBMs were responsive to the EGFR kinase inhibitor erlotinib, 7^{gain} GBMs were concurrent with overexpression of MET and HGF that may provide a more common mechanism for cell-autonomous activation of the MET signaling pathway [47]. Thus more potentials of Chr17 gain should be explored in the future. Besides, we found different frequencies of Chr17q22-23 amplification between gynecologic tumors and gastrointestinal tumors. This was in line with a previous survey that Chr17q22-23 amplifications were found in 15% of 3520 specimens of different tumor categories, in which tumors originated in the lung, mammary gland and soft tissue were the most affected. Moreover, gain of this region has been associated with poor prognosis in breast cancer [39]. In light of this, different treatment strategies may be implied in terms of gynecologic tumors and gastrointestinal tumors.

Responses to anti-HER2 therapies in HER2-amplified tumors of different histology may intrinsically be different, however, considerably various responses can even be seen in a single tumor type. According to the experience in breast cancer, HER2-target therapeutic responses were associated with different subtype status [12]. The four intrinsic subtypes of breast cancer varied in both clinical outcomes and responses to anti-HER2 therapies, in which HER2-enriched subtype exhibits the best response [8–10]. According to our study, we confirmed HER2-positive tumors were separated into four intrinsic subtypes with different fractions, consistent with a previous study [48]. HER2-enriched subtype showed the best potential responding to anti-HER2 therapies, for it harbored highest fractions of HER2-amplification or -overexpression in all levels and was characterized by vigorous metabolic activity. Besides, we found that HER2 signaling pathway was a central pathway in HER2-enriched subtype, thus HER2-positive tumors of other subtypes may not all be driven by the HER2 signaling pathway. In regard of this, more detailed molecular features are required to tailor the treatment for each patient so as to maximize the benefit and avoid overtreatment.

Clinical trials have demonstrated that not all clinical HER2-positive cases benefit from trastuzumab, such as basal-like tumors [49]. This further highlights that knowing HER2 status is not enough and molecular profiles should also be taken into consideration. In our work, we included all of 1818 significant DEGs between HER2E subtype and other counterparts of breast cancer as features and then harnessed OCLR algorithm to capture a HER2-enriched expression pattern. The HER2 index built on the weighted signatures showed satisfactory performance to distinguish tumors with HER2-enriched expression pattern in both TCGA and external datasets. The large panel of features allows the HER2-signatures to identify pathways that contain many co-regulated genes but with small individual effects, thereby preserving the interaction among genes as possible for better assessment in pan-cancer. The fgsea results of 1818-gene signature demonstrated that gene sets involved in cell proliferation and active immune response were also positively enriched besides HER2-related pathways, suggesting that this aggregated signature represented an overall transcriptional pattern taking both tumor and microenvironment into account. Of note, the negative enrichments in fgsea do not imply the absence of certain signals in tumors of HER2-enriched subtype, but rather that these pathways are lower relative to other subtypes. This was consistent with a study that proved nuclear and cytosolic accumulation of beta-catenin, a read-out of Wnt pathway activation, was enriched in basal-like breast cancers [50]. Another study clarified that TNF- α overexpression can turn trastuzumab-sensitive cells and tumors into resistant ones through inducing upregulation of MUC4 that reduced trastuzumab binding to

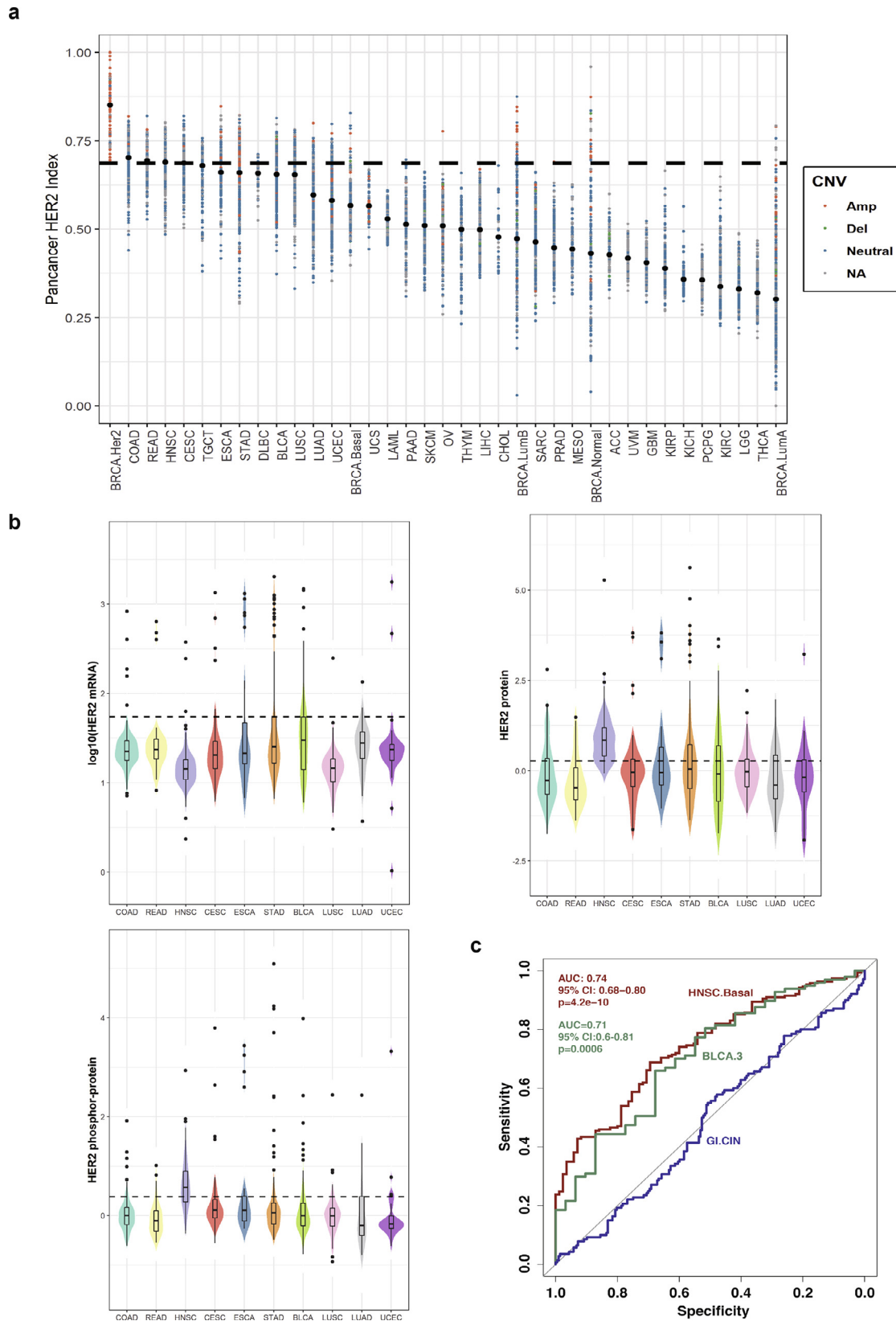


Fig. 6. Evaluation of the similarity with HER2 expression pattern across pan-cancer tumor types and subtypes. a. Comparison of HER2 expression pattern assessed by HER2 index in 33 tumor types. HER2-CNV status is labeled in which red for “Amp”, green for “Del”, blue for “Neutral” and grey for missing data. The medians of the index are labeled as black dots. b. The multi-omics feature of HER2 in the samples with higher index in ten top scored HER2-aberrant tumor types. The cutoff for log10(HER2 mRNA) (1.74), HER2 protein (0.274) and phosphor-protein (0.383) are labeled as dash lines in the three graphs respectively. c. ROC analysis. BLCA.3 and HNSC.Basal could be identified by classifiers using HER2 index.

Table 2

Frequencies of samples with both HER2 amplification/overexpression and HER2-enriched transcriptional pattern across 10 HER2-aberrant tumor types.

Cancer types	Sample size	Amp	HER2 mRNA Over.	HER2 protein & phosphor-protein Over.	HER2 alterations (Amp or protein over.)	Freq.
COAD	456	13	5	12	21	4.6%
READ	166	7	3	4	7	4.2%
HNSC	500	5	3	58	60	12.0%
CESC	304	8	8	10	13	4.3%
ESCA	161	9	7	6	10	6.2%
STAD	375	38	23	18	42	11.2%
BLCA	408	17	23	13	24	5.9%
LUSC	501	7	1	3	10	2.0%
LUAD	513	4	3	6	8	1.6%
UCEC	543	3	2	4	5	0.9%

COAD: Colon adenocarcinoma; READ: Rectum adenocarcinoma; HNSC: Head and Neck squamous cell carcinoma; CESC: Cervical squamous cell carcinoma and endocervical adenocarcinoma; ESCA: Esophageal carcinoma; STAD: Stomach adenocarcinoma; BLCA: Bladder Urothelial Carcinoma; LUSC: Lung squamous cell carcinoma; LUAD: Lung adenocarcinoma; UCEC: Uterine Corpus Endometrial Carcinoma; Amp: amplification; Over.: overexpression; Freq.: frequency.

its epitope and impaired ADCC [51], indicating the relative lower level of TNF- α signaling in tumors of HER2-enriched subtype may partially contribute to its better response to trastuzumab.

Validating our index in two GEO datasets of HER2-positive BRCA patients, we found that the HER2 index acted as an independent predictor favorable for the pCR rate and RFS of patients receiving trastuzumab-contained neoadjuvant and adjuvant regimens respectively, which was consistent with the predictive value reported of HER2-enriched subtype [11-14]. Given that part of our weighted HER2 signatures were overlapped with other indices selected, the observed stability and superiority of our index in pCR prediction could be attributed to a refined aggregation of multiple predictive pathways. A further evaluation of our index in pan-cancer cell lines showed a stronger correlation with HER2 dependency score than that with the sensitivity of pan-HER inhibitors, though both were significant. As pan-HER inhibitors also targets EGFR and ERBB3 besides HER2, this finding may suggest that our HER2 index was more suitable to identify the responders of treatment that targets HER2 specifically. It is notable that cell lines of different primary tumor types were mostly scored between 0.2 and 0.6 by our index which was distinct from the pan-cancer landscape exhibited in TCGA samples. Such mismatch might at least partially be explained by the transcriptomic discrepancies between bulk tissue and cell lines. As our index was trained to assess the overall expression pattern of the tissue samples, some of the weighted features reflected the condition of tumor stroma and could be omitted while applied to cell line data.

The HER2 index failed to obtain significance in multiple tumor types of TCGA, which could be due to the fact that HER2-targeted therapies have not been approved for use in the perioperative setting for tumors of different tissue-of-origin except BRCA. The predictive capability over response to HER2 inhibitor may not be fully reflected by prognostic discrimination in the population without corresponding treatment. Despite this, the index still showed a significant correlation with worse survival in LUAD in both TCGA and GEO cohorts, which suggested that more benefit might be achieved by HER2-targeted therapy in this tumor type.

Pan-cancer analysis of HER2 index revealed various relations with HER2 expression among different cancers and within each type of cancer. HER2-amplified tumors and ten of the thirteen HER2-aberrant cancers (Pan-GI cancers, HNSC, CESC, BLCA, LUSC, LUAD and UCEC) generally exhibited higher HER2 index. In recent years, emerging trials exploring the potential efficacy of HER2 targeted therapy in colorectal tumors [52,53], non-small cell lung cancer [54,55] and bladder cancer [56,57] with HER2 alterations (amplification, overexpression and mutations) exhibited variable responses, some of which are impressive. Furthermore, the sample sizes of these studies are small and the criteria for HER2-positive status are different from each other even in the same tumor type. It is still unknown whether and what kind of HER2 alterations are relevant

oncogenic drivers in pan-cancer tumor types, such as in NSCLC [58]. Thus criteria for more precise selection of patients to receive HER2-targeted therapies is urgently needed. Based on the analysis of BRCA, we tried to combine transcriptional pattern to HER2 alterations in order to predict the response to HER2 targeted therapy more efficiently. We observed that 0.9% to 12.0% of tumors across HER2-aberrant tumor types showed consistent HER2 amplification or overexpression with HER2-enriched transcriptional pattern, which were more likely to benefit from HER2-targeted therapy; The frequencies were lower than that of HER2 alterations reported across pan-cancer types [58]. The findings above suggested that therapeutics for HER2 may have potential value in a certain population of gastrointestinal tumors, HNSC, NSCLC, BLCA, CESC and UCEC identified by transcriptional pattern and HER2 alterations. Additionally, the discordance between high index and absence of HER2 amplifications and overexpression in some samples may be explained by activating HER2 mutations as in NSCLC [58] or alternative pathway activated in HER2-enriched expression pattern, such as KRAS mutation [53] or AR signaling [41].

Two subtypes, including HNSC.Basal and BLCA.3, could be classified by HER2 index classifier with good performance. This result agreed with a previous study that discovered connections between breast cancer and bladder cancer, in which HER2-enriched breast signature matched best with the BLCA.3 subtype [29]. Previous study showed that HER2-amplification or mRNA overexpression were rare in HNSC, but HER2 protein (85.85%) and HER2 phospho-protein level (66.04%) were largely overexpressed. Neither HER2-amplification nor overexpressed mRNA, protein or phosphorylated protein was an independent predictor of overall survival (OS) [59,60]. Currently, HER2 hasn't been regarded as a drug-target in HNSC tumors, but preclinical evidence suggests that, as a co-target of EGFR, HER2 may augment cetuximab responses and overcome therapeutic resistance [60]. Therefore, anti-HER2 therapies may be promising in these two subtypes of BLCA and HNSC. However, more studies are required to further validate these statistic-driven assumptions in the future.

In our work, we clarified the landscape of multi-omics features of HER2 status in pan-cancer and constructed a HER2 index assessing the HER2-enriched expression pattern in pan-cancer tumor types. Providing stable and superior performance in predicting the sensitivity of HER2-targeted therapies both in breast tumor tissue and pan-cancer cell lines, our index could potentially act as a pan-cancer predictive biomarker. Assessed by the combination of HER2 index and HER2 alterations, a certain population of gastrointestinal tumors, HNSC, NSCLC, BLCA, CESC and UCEC were identified which may benefit from therapeutics for HER2 target, of which BLCA.3 and HNSC.Basal are promising subtypes. More randomized trials are needed to confirm these findings, exploring criteria to refine the target population for anti-HER2 therapies in pan-cancer tumor types.

Contributors

Ziteng Li and Siyuan Chen made substantial contributions to the study design, collection and analysis of data and the writing of the article. Wanjing Feng, and Yixiao Luo participated in drafting and revising the article critically for important intellectual content. Hongyan Lai, Qin Li refined the data analysis. Bingqiu Xiu, Yuchen Li, Yan Li were involved in revising the article. Xiaodong Zhu and Shenglin Huang contributed to the study design and the final approval of the version to be published. All authors have read and approved of final manuscript.

Data Sharing Statement

The datasets generated and/or analysed during the current study are available in the TCGA database (<https://portal.gdc.cancer.gov/>); the GEO database (<https://www.ncbi.nlm.nih.gov/gds/?term=>); dependency scores and genomic data of cancer cell lines were available at the depmap database (<https://depmap.org/portal/download/>); annotations of primary disease sites and subtypes of cancer cell lines were available at the CCLE database (<https://portals.broadinstitute.org/ccle/data>).

Declaration of Competing Interest

The authors declare that they have no competing interests.

Acknowledgements

This work was funded by The National Key Research and Development Program of China (2017YFC1308900); and Clinical Research and Cultivation Project of Shanghai ShenKang Hospital Development Center (Grant No. SHDC12017X01) granted to Xiaodong Zhu. The funders have no roles in study design, data collection, data analysis, interpretation or the writing of this report.

Supplementary materials

Supplementary material associated with this article can be found, in the online version, at [doi:10.1016/j.ebiom.2020.103074](https://doi.org/10.1016/j.ebiom.2020.103074).

References

- [1] Bang YJ, Van Cutsem E, Feyereislova A, Chung HC, Shen L, Sawaki A, et al. Trastuzumab in combination with chemotherapy versus chemotherapy alone for treatment of HER2-positive advanced gastric or gastro-oesophageal junction cancer (ToGA): a phase 3, open-label, randomised controlled trial. *Lancet (Lond, Engl)* 2010;376(9742):687–97.
- [2] Slamon DJ, Leyland-Jones B, Shak S, Fuchs H, Paton V, Bajamonde A, et al. Use of chemotherapy plus a monoclonal antibody against HER2 for metastatic breast cancer that overexpresses HER2. *N Engl J Med* 2001;344(11):783–92.
- [3] Oh DY, Bang YJ. HER2-targeted therapies - a role beyond breast cancer. *Nat Rev Clin Oncol* 2019.
- [4] Yarden Y, Sliwkowski MX. Untangling the ErbB signalling network. *Nat Rev Mol Cell Biol* 2001;2(2):127–37.
- [5] Wolff AC, Hammond MEH, Allison KH, Harvey BE, Mangu PB, Bartlett JMS, et al. Human epidermal growth factor receptor 2 testing in breast cancer: American Society of Clinical Oncology/College of American Pathologists Clinical Practice Guideline Focused Update. *J Clin Oncol* 2018;36(20):2105–22.
- [6] Triulzi T, Bianchi GV, Tagliabue E. Predictive biomarkers in the treatment of HER2-positive breast cancer: an ongoing challenge. *Futur Oncol (Lond, Engl)* 2016;12(11):1413–28.
- [7] Perou CM, Sørlie T, Eisen MB, van de Rijn M, Jeffrey SS, Rees CA, et al. Molecular portraits of human breast tumours. *Nature* 2000;406(6797):747–52.
- [8] Sørlie T, Perou CM, Tibshirani R, Aas T, Geisler S, Johnsen H, et al. Gene expression patterns of breast carcinomas distinguish tumor subclasses with clinical implications. *PNAS* 2001;98(19):10869–74.
- [9] Sørlie T, Tibshirani R, Parker J, Hastie T, Marron JS, Nobel A, et al. Repeated observation of breast tumor subtypes in independent gene expression data sets. *PNAS* 2003;100(14):8418–23.
- [10] Parker JS, Mullins M, Cheang MC, Leung S, Voduc D, Vickery T, et al. Supervised risk predictor of breast cancer based on intrinsic subtypes. *J Clin Oncol* 2009;27(8):1160–7.
- [11] Carey LA, Berry DA, Cirincione CT, Barry WT, Pitcher BN, Harris LN, et al. Molecular Heterogeneity and Response to Neoadjuvant Human Epidermal Growth Factor Receptor 2 Targeting in CALGB 40601, a Randomized Phase III Trial of Paclitaxel Plus Trastuzumab With or Without Lapatinib. *J Clin Oncol* 2016;34(6):542–9.
- [12] Llombart-Cussac A, Cortés J, Paré L, Galván P, Bermejo B, Martínez N, et al. HER2-enriched subtype as a predictor of pathological complete response following trastuzumab and lapatinib without chemotherapy in early-stage HER2-positive breast cancer (PAMELA): an open-label, single-group, multicentre, phase 2 trial. *Lancet Oncol* 2017;18(4):545–54.
- [13] Fumagalli D, Venet D, Ignatiadis M, Azim HA, Maetens M, Rothé F, et al. RNA sequencing to predict response to neoadjuvant anti-HER2 therapy: a secondary analysis of the NeoALTTO randomized clinical trial. *JAMA Oncol* 2017;3(2):227–34.
- [14] Perez EA, Ballman KV, Mashadi-Hosseini A, Tenner KS, Kachergus JM, Norton N, et al. Intrinsic subtype and therapeutic response among HER2-positive breast tumors from the NCCCTG (Alliance) N9831 trial. *J Natl Cancer Inst* 2017;109(2).
- [15] Colaprico A, Silva TC, Olsen C, Garofano L, Cava C, Garolini D, et al. TCGAbiolinks: an R/Bioconductor package for integrative analysis of TCGA data. *Nucleic Acids Res* 2016;44(8):e71–e.
- [16] Mermel CH, Schumacher SE, Hill B, Meyerson ML, Beroukhi R, Getz G. GISTIC2.0 facilitates sensitive and confident localization of the targets of focal somatic copy-number alteration in human cancers. *Genome Biol* 2011;12(4):R41–R.
- [17] Beroukhi R, Mermel CH, Porter D, Wei G, Raychaudhuri S, Donovan J, et al. The landscape of somatic copy-number alteration across human cancers. *Nature* 2010;463(7283):899–905.
- [18] Samur MK. RTCGAToolbox: a new tool for exporting TCGA Firehose data. *PLoS One* 2014;9(9):e106397–e.
- [19] Davis S, Meltzer PS. GEOquery: a bridge between the Gene Expression Omnibus (GEO) and BioConductor. *Bioinformatics* 2007;23(14):1846–7.
- [20] Yang W, Soares J, Greninger P, Edelman EJ, Lightfoot H, Forbes S, et al. Genomics of Drug Sensitivity in Cancer (GDSC): a resource for therapeutic biomarker discovery in cancer cells. *Nucleic Acids Res* 2013;41(Database issue):D955–D61.
- [21] Meyers RM, Bryan JG, McFarland JM, Weir BA, Sizemore AE, Xu H, et al. Computational correction of copy number effect improves specificity of CRISPR-Cas9 essentiality screens in cancer cells. *Nat Genet* 2017;49(12):1779–84.
- [22] Broad D. DepMap Achilles 19Q1 Public2019.
- [23] Barretina J, Caponigro G, Stransky N, Venkatesan K, Margolin AA, Kim S, et al. The Cancer Cell Line Encyclopedia enables predictive modelling of anticancer drug sensitivity. *Nature* 2012;483:603.
- [24] The Cancer Cell Line Encyclopedia C, Stransky N, Ghandi M, Kryukov GV, Garraway LA, Lehar J, et al. Pharmacogenomic agreement between two cancer cell line data sets. *Nature* 2015;528:84.
- [25] Liberzon A, Subramanian A, Pinchback R, Thorvaldsdóttir H, Tamayo P, Mesirov JP. Molecular signatures database (MSigDB) 3.0. *Bioinformatics* 2011;27(12):1739–40.
- [26] Subramanian A, Tamayo P, Mootha VK, Mukherjee S, Ebert BL, Gillette MA, et al. Gene set enrichment analysis: a knowledge-based approach for interpreting genome-wide expression profiles. *Proc Natl Acad Sci* 2005;102:15545–50.
- [27] Hänzelmann S, Castelo R, Guinney J. GSEA: gene set variation analysis for microarray and RNA-Seq data. *BMC Bioinformatics* 2013;14(1):7.
- [28] Bastien RR, Á Rodríguez-Lescure, Ebbert MT, Prat A, Munárriz B, Rowe L, et al. PAM50 breast cancer subtyping by RT-qPCR and concordance with standard clinical molecular markers. *BMC Med Genom* 2012;5:44.
- [29] Sokolov A, Paull EO, Stuart JM. One-class detection of cell states in tumor subtypes. *Pac Symp Biocomput Pac Symp Biocomput* 2016;21:405–16.
- [30] Malta TM, Sokolov A, Gentles AJ, Burzykowski T, Poisson L, Weinstein JN, et al. Machine learning identifies stemness features associated with oncogenic dedifferentiation. *Cell* 2018;173(2):338–54.
- [31] Korotkevich G, Sukhov V, Sergushichev A. Fast gene set enrichment analysis. *bioRxiv* 2019:060012.
- [32] Parker JS, Mullins M, Cheang MCU, Leung S, Voduc D, Vickery T, et al. Supervised risk predictor of breast cancer based on intrinsic subtypes. *J Clin Oncol* 2009;27(8):1160–7.
- [33] Wu VT, Kiriazov B, Koch KE, Gu VW, Beck AC, Borcherding N, et al. A gene signature is predictive of outcome in HER2-positive breast cancer. *Mol Cancer Res* 2020;18(1):46–56.
- [34] Risi E, Biagioni C, Benelli M, Migliaccio I, McCartney A, Bonechi M, et al. An RB-1 loss of function gene signature as a tool to predict response to neoadjuvant chemotherapy plus anti-HER2 agents: a substudy of the NeoALTTO trial (BIG 1-06). *Ther Adv Med Oncol* 2019;11:1758835919891608.
- [35] Liu JC, Voisin V, Bader GD, Deng T, Puszta I, Symmans WF, et al. Seventeen-gene signature from enriched Her2/Neu mammary tumor-initiating cells predicts clinical outcome for human HER2+ERα- breast cancer. *Proc Natl Acad Sci USA* 2012;109(15):5832–7.
- [36] Sonnenblick A, Brohée S, Fumagalli D, Vincent D, Venet D, Ignatiadis M, et al. Constitutive phosphorylated STAT3-associated gene signature is predictive for trastuzumab resistance in primary HER2-positive breast cancer. *BMC Med* 2015;13:177.
- [37] Sonnenblick A, Salmon-Divon M, Salgado R, Dvash E, Pondé N, Zahavi T, et al. Reactive stroma and trastuzumab resistance in HER2-positive early breast cancer. *Int J Cancer* 2020;147(1):266–76.
- [38] Dieci MV, Prat A, Tagliafico E, Paré L, Ficarra G, Bisagni G, et al. Integrated evaluation of PAM50 subtypes and immune modulation of pCR in HER2-positive breast cancer patients treated with chemotherapy and HER2-targeted agents in the CherLOB trial. *Ann Oncol* 2016;27(10):1867–73.

- [39] Santarius T, Shipley J, Brewer D, Stratton MR, Cooper CS. A census of amplified and overexpressed human cancer genes. *Nat Rev Cancer* 2010;10:59.
- [40] Newton Y, Novak AM, Swatoski T, McColl DC, Chopra S, Graim K, et al. Tumor-Map: exploring the molecular similarities of cancer samples in an interactive portal. *Cancer Res* 2017;77(21):e111.
- [41] Daemen A, Manning G. HER2 is not a cancer subtype but rather a pan-cancer event and is highly enriched in AR-driven breast tumors. *Breast Cancer Research BCR* 2018;20(1):8.
- [42] Downs-Kelly E, Yoder BJ, Stoler M, Tubbs RR, Skacel M, Grogan T, et al. The influence of polysomy 17 on HER2 gene and protein expression in adenocarcinoma of the breast. *Am J Surg Pathol* 2019;29(9):1221–7.
- [43] Cocco E, Lopez S, Santin AD, Scaltriti M. Prevalence and role of HER2 mutations in cancer. *Pharmacol Ther* 2019;199:188–96.
- [44] Pahuja KB, Nguyen TT, Jaiswal BS, Prabhash K, Thaker TM, Senger K, et al. Actionable activating oncogenic ERBB2/HER2 transmembrane and juxtamembrane domain mutations. *Cancer Cell* 2018;34(5):792–806.
- [45] Chmielecki J, Ross JS, Wang K, Frampton GM, Palmer GA, Ali SM, et al. Oncogenic alterations in ERBB2/HER2 represent potential therapeutic targets across tumors from diverse anatomic sites of origin. *Oncologist* 2015;20(1):7–12.
- [46] Zehir A, Benayed R, Shah RH, Syed A, Middha S, Kim HR, et al. Erratum: Mutational landscape of metastatic cancer revealed from prospective clinical sequencing of 10,000 patients. *Nat Med* 2017;23(8):1004.
- [47] Beroukhim R, Getz G, Nghiemphu L, Barretina J, Hsueh T, Linhart D, et al. Assessing the significance of chromosomal aberrations in cancer: methodology and application to glioma. *Proc Natl Acad Sci USA* 2007;104(50):20007–12.
- [48] Wallden B, Storhoff J, Nielsen T, Dowidar N, Schaper C, Ferree S, et al. Development and verification of the PAM50-based Prosigna breast cancer gene signature assay. *BMC Med Genet* 2015;8:54.
- [49] Intrinsic Subtype and Therapeutic Response Among HER2-Positive Breast Tumors from the NCCCTG (Alliance) N9831 Trial. *J Natl Cancer Inst* 2017.
- [50] Khrantsov AI, Khrantsova GF, Tretiakova M, Huo D, Olopade OI, Goss KH. Wnt/beta-catenin pathway activation is enriched in basal-like breast cancers and predicts poor outcome. *Am J Pathol* 2010;176(6):2911–20.
- [51] Mercogliano MF, De Martino M, Venturutti L, Rivas MA, Proietti CJ, Inurrigarro G, et al. TNF α -Induced Mucin 4 Expression Elicits Trastuzumab Resistance in HER2-Positive Breast Cancer. *Clin Cancer Res* 2017;23(3):636–48.
- [52] Sartore-Bianchi A, Trusolino L, Martino C, Bencardino K, Lonardi S, Bergamo F, et al. Dual-targeted therapy with trastuzumab and lapatinib in treatment-refractory, KRAS codon 12/13 wild-type, HER2-positive metastatic colorectal cancer (HERACLES): a proof-of-concept, multicentre, open-label, phase 2 trial. *Lancet Oncol* 2016;17(6):738–46.
- [53] Meric-Bernstam F, Hurwitz H, Raghav KPS, McWilliams RR, Fakih M, VanderWalde A, et al. Pertuzumab plus trastuzumab for HER2-amplified metastatic colorectal cancer (MyPathway): an updated report from a multicentre, open-label, phase 2a, multiple basket study. *Lancet Oncol* 2019;20(4):518–30.
- [54] Peters S, Stahel R, Bubendorf L, Bonomi P, Villegas A, Kowalski DM, et al. Trastuzumab Emtansine (T-DM1) in Patients with Previously Treated HER2-overexpressing metastatic non-small cell lung cancer: efficacy, safety, and biomarkers. *Clin Cancer Res* 2019;25(1):64–72.
- [55] Wang Y, Jiang T, Qin Z, Jiang J, Wang Q, Yang S, et al. HER2 exon 20 insertions in non-small-cell lung cancer are sensitive to the irreversible pan-HER receptor tyrosine kinase inhibitor pyrotinib. *Ann Oncol: Off J Eur Soc Med Oncol* 2019;30(3):447–55.
- [56] Hussain MHA, MacVicar GR, Petrylak DP, Dunn RL, Vaishampayan U, Lara PN, et al. Trastuzumab, paclitaxel, carboplatin, and gemcitabine in advanced human epidermal growth factor receptor-2/neu-positive urothelial carcinoma: results of a multicenter phase II National Cancer Institute trial. *J Clin Oncol* 2007;25(16):2218–24.
- [57] Powles T, Huddart RA, Elliott T, Sarker S-J, Ackerman C, Jones R, et al. Phase III, double-blind, randomized trial that compared maintenance lapatinib versus placebo after first-line chemotherapy in patients with human epidermal growth factor receptor 1/2-Positive Metastatic Bladder Cancer. *J Clin Oncol* 2017;35(1):48–55.
- [58] Jebbink M, de Langen AJ, Boelens MC, Monkhorst K, Smit EF. The force of HER2 - a druggable target in NSCLC? *Cancer Treat Rev* 2020;86:101996.
- [59] Khademi B, Shirazi FM, Vasei M, Doroudchi M, Gandomi B, Modjtahedi H, et al. The expression of p53, c-erbB-1 and c-erbB-2 molecules and their correlation with prognostic markers in patients with head and neck tumors. *Cancer Lett* 2002;184(2):223–30.
- [60] Pollock NI, Grandis JR. HER2 as a therapeutic target in head and neck squamous cell carcinoma. *Clin Cancer Res* 2015;21(3):526–33.